Are anticoagulant independent mechanical valves within reach—fast prototype fabrication and *in vitro* testing of innovative bi-leaflet valve models

Lawrence N. Scotten[1], Rolland Siegel[2]

[1]ViVitro Systems Inc. (VSI), Victoria, BC, Canada; [2]Lake Oswego, OR, USA

Contributions: (I) Conception and design: LN Scotten; (II) Administrative support: LN Scotten; (III) Provision of study materials: LN Scotten; (IV) Collection and assembly of data: LN Scotten; (V) Data analysis and interpretation: LN Scotten; (VI) Manuscript writing: All authors; (VII) Final approval of manuscript: All authors.

Correspondence to: Lawrence N. Scotten. Dipl. T., Director, ViVitro Systems Inc., (VSI), 6-1560 Church Avenue, Victoria, BC V8P 2H1, Canada. Email: larryscotten2@hotmail.com.

Background: Exploration for causes of prosthetic valve thrombogenicity has frequently focused on forward or post-closure flow detail. In prior laboratory studies, we uncovered high amplitude flow velocities of short duration close to valve closure implying potential for substantial shear stress with subsequent initiation of blood coagulation pathways. This may be relevant to widely accepted clinical disparity between mechanical and tissue valves vis-à-vis thrombogenicity. With a series of prototype bi-leaflet mechanical valves, we attempt reduction of closure related velocities with the objective of identifying a prototype valve with thrombogenic potential similar to our tissue valve control. This iterative design approach may find application in preclinical assessment of valves for anticoagulation independence.

Methods: Tested valves included: prototype mechanical bi-leaflet BVs (n=56), controls (n=2) and patented early prototype mechanicals (n=2) from other investigators. Pulsatile and quasi-steady flow systems were used for testing. Projected dynamic valve area (PDVA) was measured using previously described novel technology. Flow velocity over the open and closing periods was determined by volumetric flow rate/PDVA. For the closed valve interval, use was made of data obtained from quasi-steady back pressure/flow tests. Performance was ranked by a proposed thrombogenicity potential index (TPI) relative to tissue and mechanical control valves.

Results: Optimization of the prototype valve designs lead to a 3-D printed model (BV_{3D}). For the mitral/aortic site, BV_{3D} has lower TPI (1.10/1.47) relative to the control mechanical valve (3.44/3.93) and similar to the control tissue valve (ideal TPI ≤1.0).

Conclusions: Using unique technology, rapid prototyping and thrombogenicity ranking, optimization of experimental valves for reduced thrombogenic potential was expedited and simplified. Innovative mechanical valve configurations were identified that merit consideration for further development which may bring the anti-coagulation independent mechanical valve within reach.

Keywords: Prosthetic valve; thrombogenicity; flow velocities; rebound

Submitted Aug 11, 2015. Accepted for publication Aug 17, 2015.

doi: 10.3978/j.issn.2305-5839.2015.08.18

View this article at: http://dx.doi.org/10.3978/j.issn.2305-5839.2015.08.18

Introduction

Throughout the evolution of mechanical valves from ball to disk to bi-leaflet, all shared two common operating characteristics; occluder closure primarily activated by reverse blood flow and a requirement for permanent anti-vitamin K anticoagulation to minimize life-threatening thrombotic complications. Possible causes for valve thrombogenicity have been explored extensively for mechanical valves with emphasis on forward and post-closure flow detail. Our prior work strongly suggested that dynamic events close to mechanical valve closure, including rapid closure and water-hammer driven valve rebound behavior, generate flow velocities and shear rates which may contribute to the problem (1-3). The effect of high fluid velocities of short duration and resulting shear stress on human blood was recently reported by Ding and associates who stated: "it is well known that elevated shear stresses can cause platelet activation" (4). Using Leonardo^{VSI}, a unique opto-electronic subsystem integrated into our modified pulse duplicator described previously (2) and a rapid-prototyping strategy, we ranked the performance of a range of tested valves in a thrombogenicity potential index (TPI). Our prototype models were successfully evolved to produce TPIs close to that of our bioprosthetic control valve and substantially less than our mechanical control valve demonstrating that an innovative mechanical valve with tissue valve-like thrombogenic profile is feasible.

Historic overview and rationale for this study

As only fleeting glimpses of prosthetic valve motion can be seen by the unaided eye, advanced high speed digital imaging techniques have traditionally been utilized to observe valve motion detail. A simpler methodology (Leonardo^{VSI}) transcends barriers of time and space and quantified valve movement by detecting light passing through functioning test valves with a photo sensor on the other side calibrated for projected light area. Furthermore, by dividing instantaneous valve volumetric flow rate by PDVA, previously unseen crucial events close to valve closure including flow reversal, water hammer and occluder rebound revealed remarkably high spatial average regional flow velocities (RFV_{SA}) across contemporary mechanical heart valves (1-3). Of very short duration they far exceeded levels observed with tissue valves. Intense backflow velocity transients can produce shear damage of blood components thus initiating the clotting cascade (1-3). Our prior work suggested that increased regional backflow velocity (RBV_{-MAX}) infers higher shear rates and greater valve thrombogenicity (1,2). In that work, we postulated that transient backflow velocities of high magnitude across valves are a primary initiator of shear rate damage to formed blood elements deemed responsible for valve thrombogenicity. Multiple backflow impulses coincident with bouncing observed in ball valve closure in a pulse duplicator in 1966 by Davey and colleagues (5,6) appear to be the earliest published evidence of this crucial phenomenon. Inability to conveniently appreciate the magnitude and short duration of these previously hidden velocities in a laboratory or clinical setting resulted in a longstanding preoccupation with forward flow detail. This may have inhibited design modification of mechanical valves resulting in acceptance of an irreducible incidence of thrombotic and bleeding events. More than 30 years after the introduction of modern prosthetic valves, the choice of a biological or a mechanical valve in the mitral position is still the subject of debate (7,8). The principle differences between the two types of valves are finite durability for bioprostheses and thrombogenicity for mechanical prostheses with historic wide cyclic variation in preference for one type of valve versus the other. The introduction of transcatheter aortic valve replacement (TAVR) adds yet another alternative for consideration in valve selection decision-making. Although an attractive less invasive option for fragile elderly patients, an inconvenient truth associated with this technology has persisted about a high incidence of peri-prosthetic leak and the effect on morbidity and mortality has stimulated investigations into the more subtle neurologic consequences of both mechanical and bioprosthetic valve replacement (9-12). These investigations focused attention on silent neurological injury, brain lesions and cognitive decline after valve replacement. While there is no common denominator for these adverse events, activation of clotting components by the replacement valve and dislodgement of debris by manipulations during valve replacement/insertion are certainly contributory (13,14). Over time, refinement in tissue treatment technology and improved stent design has mitigated the causes for early bioprosthetic valve failure and they are currently considered suitable for aortic replacement in adults 60+ and mitral replacement 70+ (15,16). Nonetheless, the choice of an appropriate prosthesis remains complex (17,18), and the goal of a lifetime-durable anti-coagulation

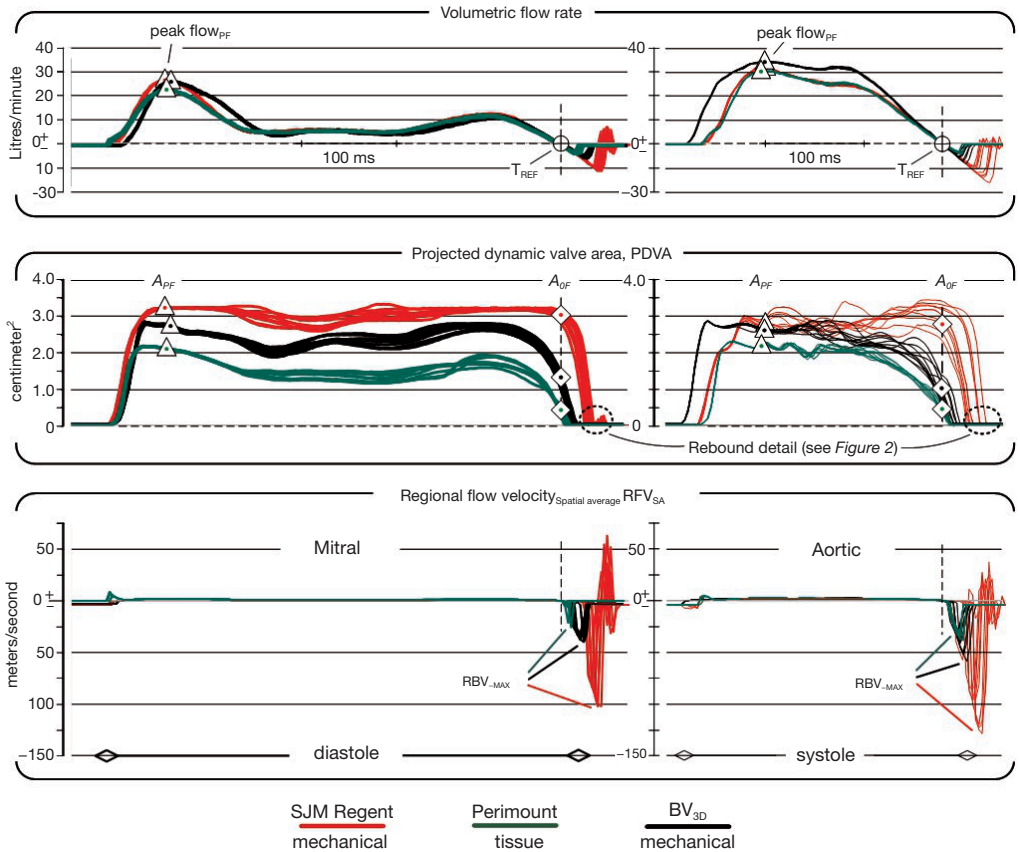

Figure 1 Mitral and aortic valve motion (PDVA) and hydrodynamic profiles (n=10 consecutive cycles). The black waveforms apply to the model BV_{3D} fast printed prototype mechanical valve and the red and green are the controls. Test conditions: heart rate 70/min, cardiac output ~5 L/min, ~peak instantaneous flow rates (diastolic 27 L/min, systolic 35 L/min), test fluid saline. Marked data point details are provided in supplementary materials. See *Figure 2* for examples of SJM rebound behavior.

independent valve challenging and elusive.

Materials and methods

Test apparatus

Valves were tested in pulsatile and quasi-steady pressure/flow systems and projected dynamic valve area (PDVA) was obtained (1,2). Pulsatile flow velocity profiles over the open and closing phases were determined (volumetric flow rate/PDVA). Accurate measurement of closed valve leakage was obtained in a quasi-steady pressure/flow apparatus calibrated with known small orifice areas (1). Valve leakage areas assigned for pulsatile test data analysis ranged between 0.02-0.04 cm^2.

Test valve details are described in the supplementary materials.

Results

Figure 1 compares waveforms for three valves tested under pulsatile flow conditions in the mitral and aortic site. *Figure 2* shows two types of valve rebound behavior; initial impact and water-hammer driven. *Figure 3* shows TPI performance. Valves with lowest TPI are considered most promising. Our significant findings are:

(I) Occluder motion is influenced by a non-linear mechanical advantage relationship; static length ratio (C_1/C_2. See *Figure S1*);

(II) Decelerating forward flow can be beneficially exploited by specific leaflet geometric parameters to induce dynamic closure force on valve occluders prior to forward flow reversal;

(III) Balancing flow induced forces on opening/closing occluders can optimize TPI as evidenced, for

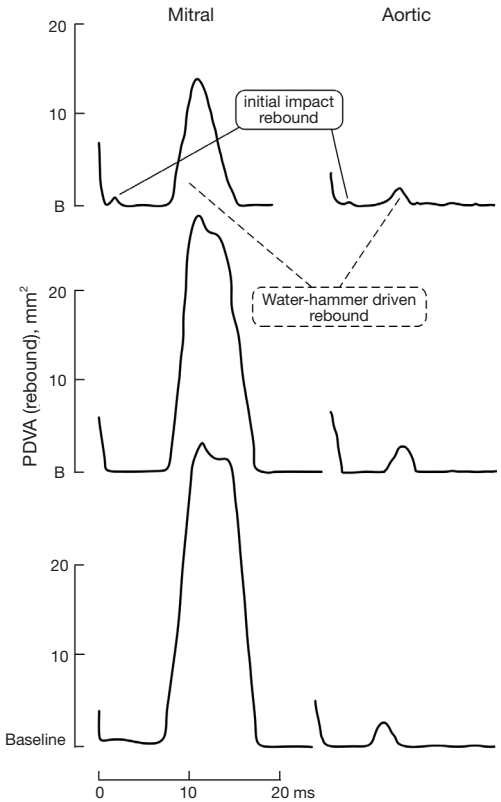

Figure 2 In mitral and aortic site, separate examples of valve rebounds for one SJM Regent valve during three non-consecutive cycles from previously published data (3). The baseline (B) is the closed valve PDVA. Analog signal bandwidth is 0-16 kHz and acquisition sampling rate 100 kHz.

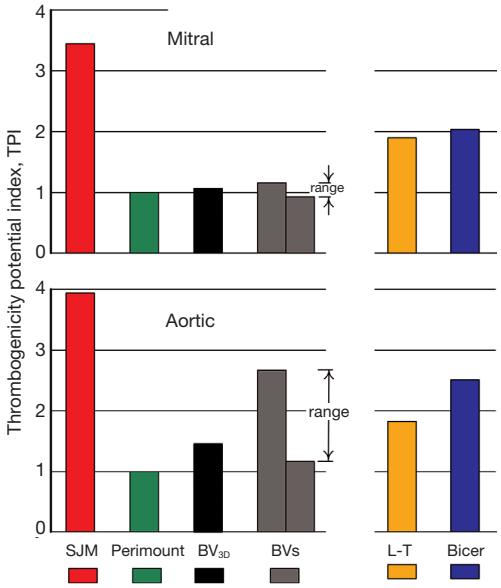

Figure 3 TPI ranking for a range of prototype BVs versus control valves in mitral and aortic positions. BVs represents highest and lowest TPI ranked valves of 55 laboratory constructed prototypes. BV_{3D} is based on a CAD drawing of the lowest ranked BVs prototype. Also compared are patented preliminary mechanical models, the tri-leaflet Lapeyre-Triflo (L-T) valve (19,20) and the bi-leaflet Bicer valve (21).

example, by specific convex leaflet curvature at the valve inflow and aileron angle parameters.

The crux of our work is supported by data in *Figure 1*.

(I) Color coded waveforms and data points A_{PF} and A_{0F} are synchronous with their respective flows;

(II) The red and black waveforms are time shifted so that zero flow rates coincide with the green waveform at the position marked T_{REF}, the cross-over point where positive flow becomes negative;

(III) Recognizing closed valve intervals when PDVA is minimal, our methodology reassigns leakage flow rate and geometric area data obtained from quasi-steady pressure/flow testing (120/80 mmHg) to the pertinent pulsatile closed valve intervals;

(IV) High magnitude short duration (transients) flow velocities (RBV_{-MAX}) close to valve closure far exceeded forward flow velocities;

(V) The highest recorded transients in the RFV_{SA} waveforms were generated by the SJM Regent™ valve (red) compared to the Perimount™ valve (green);

(VI) BV_{3D} (black) produced RFV_{SA} profiles similar to the tissue control valve.

Comparing the PDVA waveforms in the center panel of *Figure 1* (close to the end of diastole for mitral valves or systole for aortic valves), note the delayed onset of leaflet closure motion (PDVA decrease) for the SJM Regent™ whereas leaflet closure initiates earlier during the forward flow deceleration phase for the Perimount™ control valve and the BV_{3D}. A stand-alone leakage measurement system previously described (2) was used to obtain closed valve leakage area and flow rate pertinent to occluder peripheral and hidden pivot gap regions.

Forward flow deceleration response vs. reverse flow response

The significance of reverse flow versus decelerating

forward flow response (soft or tissue valve-like) closure is reflected in the lower panel of *Figure 1* showing RFV_{SA}. Reverse flow closure response appears to be an intrinsic functional deficiency of all current mechanical heart valves. In contrast, deceleration closure response for tissue valves is considered more physiologic and may be important for reduced thrombogenic potential.

Rebound behavior in vitro

In *Figure 2*, two types of rebound behavior are evident; initial and water-hammer. This behavior is typical for current mechanical heart valves. Most prominent is the water-hammer rebound in the mitral position. Initial impact rebounds are less frequent and lower amplitude but are present in both mitral and aortic positions. Rebound and its effect on PDVA profile has been previously reported (2,3,22). Water-hammer rebound causes flow oscillations that force fluid through decreasing (then transient increased) geometric flow area (PDVA) and produces distinctive spikes in the RFV profile. For the SJM valve, water-hammer rebound in the mitral position is brief in duration ≤~12 ms and can be ~22 times greater in amplitude than in the aortic position (see *Figure 2*, lower panel). This may partially explain why mitral valve implants, and mechanical valves in particular are reported as more thrombogenic than aortic valves (23,24). Cannegieter and associates (25) reported that: "The incidence rate of the (mechanical) mitral valve compared with that of the aortic valve was five times as high for thrombosis and about 1.5 times as high for embolism." Interestingly, rebound peak flow (PF) velocities of ~120 m/s have been reported by Krishnan and associates in a two-dimensional dynamic simulation study of bi-leaflet mitral valve closure (26). In our study, Perimount^{TM} and BV_{3D}, rebound spikes and RBV_{-MAX} are moderate and did not exceed ~50 m/s. For the SJM Regent^{TM} it reaches RBV_{-MAX} of ~125 m/s which implies a high thrombogenic potential. *In vitro*, a tissue valve-like "soft" closing profile along with either complete sealing or optimized closed leakage area are important for minimizing water-hammer driven rebound and subsequent RFV_{SA} transients and may be an essential dynamic characteristic for low thrombogenic function. The degree to which water-hammer rebound is affected by ventricle viscoelasticity could be the subject of future study using the adjustable compliance available with the VIA component.

Thrombogenicity ranking

Data from these experiments was organized in a rational order representing gradations of higher/lower thrombogenicity (TPI). In *Figure 3* the TPI facilitates a comparison of a number of prototype BVs (n=56), and the clinical control valves [St Jude Medical, Regent^{TM} mechanical (SJM); Edwards Perimount^{TM} tissue]. In this TPI ranking, the lowest in range of the BVs outperformed the SJM control valve by a factor of ~3.1 times in the aortic site and ~3.8 times in the mitral. A small discrepancy in TPI between BV_{3D} and best BV model may be related, in part, to lower BV_{3D} material density. The calculation method for determining TPI is given in supplementary materials.

Quantitative assessment of clinical valve thrombogenicity is currently unavailable and only qualitative opinions are offered on this subject. There is however an undeniable major disparity between tissue and mechanical valves evidenced *in vitro* and previously reported (1-3). Therefore, we submit that TPI may serve as a proportional surrogate to clinical valve thrombogenicity but we acknowledge that future translational studies are required to validate this hypothesis.

In light of our prior published work, our intuition regarding basic mechanical valve design favored multi-leaflet and central opening. A preferred model provides a tent-like closure where the angle of motion of each leaflet from full closed to open is small (e.g., ~22°) which allows completion of closure in less time and may mitigate rebound. Similar rationale for innovative mechanical heart valves had been proposed by Lapeyre (19,20) and Bicer (21). The 56 laboratory constructed prototype valves are represented in *Figure 3* as BVs include one BV_{3D} model (black bars). These prototype models (BVs) were consistent with the basic tenets of previous patented mechanical valves (L-T and Bicer) but incorporated variations of leaflet detail resulting in a range of TPI results (grey bars representing High/Low range are shown in *Figure 3*). All models were tested and TPI was the objective criteria for optimization. The BV_{3D} valve is based on a CAD drawing of the laboratory constructed valve with the lowest TPI ranking. With the advantage of fast prototype construction and our *in vitro* thrombogenicity ranking methodologies, we were able to assess the dynamic effects of a significant number of geometric parameters in a relatively short time.

For the BV_{3D} prototype model, the pivot axis location and pronounced leaflet aileron angle (Di. See *Figure S1*) appear to enhance deceleration closure but may restrict

flow through the two minor orifices. In writing of problems associated with early model Björk-Shiley valves (Delrin, Spherical-Radial), Yoganathan and associates reported that decreased PF velocity and lower peak shear stress on the sewing ring adjacent to the minor flow orifice contributed to thrombus and pannus formation (27). Changing the disk configuration to convexo-concave and relocating the pivot axis increased minor orifice flow and was considered to have mitigated the thrombus/pannus problem (28). This major/minor flow disparity may be germane to the BV_{3D} design requiring further valve modification and study.

With Leonardo Technology for evidence based objective assessment of thrombogenic potential in novel mechanical valve designs, we believe this study provides an experimental pathway for development of less thrombogenic valve implants. As shown in *Figure 1*, this work suggests that with further modifications, specific prototype valve models may virtually replicate tissue control valve closure dynamics.

Future preclinical considerations and development

Formation of thrombus using human blood in an *in vitro* system described as a "Device Thrombogenicity Emulator" represents a hybrid method for comparing valve to valve thrombogenic potential (29). Additionally, a variety of computational fluid dynamics (CFD) methods as well as digital particle imaging velocimetry (DPIV) have contributed to improved understanding of the sources of thrombogenicity in mechanical heart valves (30,31). The value of simulation is contingent however on how accurately it can predict physical reality, and how quickly it can produce results. To date, none of these *in vitro* or numerical methods have produced data that correlates directly with mechanical valve clinical thrombogenicity. Ranking of novel valves where TPI is based on comparison with both mechanical and bioprosthetic controls may be a more accurate and realistic *in vitro* method of predicting thrombogenic activity after valve replacement in humans.

A variety of pre-clinical strategies have been employed to indicate safety of innovative valves for human implantation. These included high speed cycling for durability and pulse duplicator analysis for hydrodynamic parameters. Chronic implantation in a wide range of animal models has been utilized to predict potential clinical thrombogenicity. Currently, with over 35 years of historic data, sheep are considered the preferred model with implant data on almost all heart valves now in clinical service (Bianco R, 2015, unpublished data). A novel variant of a pre-clinical animal study is placement of mechanical valves in the pulmonic position in sheep and monitoring the interval to onset of thrombosis (32,33). The proponents of this method state: "*The model allows us to compare the thrombogenic potential of different mechanical valve types, while it can also serve as a test for new therapeutic or diagnostic tools for mechanical valve thrombosis.*" (33).

Limitations

More realistic prototypes with improved geometric leakage (GAP) area control may be needed for final optimization:

(I) Total closed valve GAP areas can be determined/adjusted using accurate quasi-steady pressure/flow leak testing (initial target ~0.04 cm^2);
(II) Hypothesis: valve inflow patterns are affected by prior cycle backflows thus influencing valve motion during the open/closing phases. If confirmed, it emphasizes the importance of more detailed and accurate prototypes;
(III) At present, there is a lack of independent confirmation of our results or correlation with clinical studies;
(IV) The impact of leaflet material density could be determined by testing valves with identical leaflets from materials of different densities. This might disclose whether more accurate prototype models fabricated from materials with density that more closely approximates clinical quality valves are necessary for desired leaflet motion (e.g., effect on occluder rebound);
(V) Refined models with precision fit-up tolerances are needed for subsequent study of rebound behavior and delineation of a 3-D printed prototype;
(VI) An appropriate pivot design is required.

Strengths

(I) Stable reference time for waveform synchronization was found by using T_{REF};
(II) Specific modifications produced data that resulted in a thrombogenicity ranking closely approximating that of our clinical bioprosthetic valve control (Edwards Perimount^{TM});
(III) A mechanical valve design with potential for clinical application can be identified and characterized utilizing our *in vitro* methods and ranking system including detailed rebound behavior;

(IV) Results suggest that a mechanical valve can be designed with reduced thrombogenic potential comparable to clinically well established tissue valves.

Conclusions

Our prior work strongly suggested that dynamic events close to valve closure constitute an important, perhaps primary contribution to valve thrombogenicity. Together with rapid prototyping and a thrombogenicity ranking system, Leonardo Technology offers insight into both forward and closure valve dynamics. It is a simple practical method for evaluation of advanced valve designs that may have potential for anticoagulation independent function. We submit that TPI may serve as a proportional surrogate to clinical valve thrombogenicity but we acknowledge that future translational studies are required to validate this hypothesis. This work suggests that with further modifications, specific prototype valve models may virtually replicate tissue control valve closure dynamics.

Acknowledgements

The authors are grateful to the following for their generous contributions to this manuscript: Aurelio Chaux (MD), Richard Gray (MD), Jon Stupka (BS), P. Eng, Boyce Griffith (PhD), James Dutton (MD).

Footnote

Conflicts of Interest: The authors have no conflicts of interest to declare.
Financial Disclosure: ViVitro Systems Inc. (VSI).

References

1. Scotten LN, Siegel R. Thrombogenic potential of transcatheter aortic valve implantation with trivial paravalvular leakage. Ann Transl Med 2014;2:43.
2. Scotten LN, Siegel R. Importance of shear in prosthetic valve closure dynamics. J Heart Valve Dis 2011;20:664-72.
3. Scotten LN, Walker DK. New laboratory technique measures projected dynamic area of prosthetic heart valves. J Heart Valve Dis 2004;13:120-32; discussion 132-3.
4. Ding J, Chen Z, Niu S. Quantification of shear-induced platelet activation: High shear stresses for short exposure time. Artificial Organs 2015;39:576-83.
5. Davey TB, Kaufman B, Smeloff, EA. Pulsatile flow studies of prosthetic heart valves. J Thorac Cardiovasc Surg 1966;51:264-7.
6. Smeloff EA, Huntley AC, Davey TB, et al. Comparative study of prosthetic heart valves. J Thorac Cardiovasc Surg 1966;52:841-8.
7. Ribeiro AH, Wender OC, de Almeida AS, et al. Comparison of clinical outcomes in patients undergoing mitral valve replacement with mechanical or biological substitutes: a 20 years cohort. BMC Cardiovasc Disord 2014;14:146.
8. Suri RM, Schaff HV. Selection of aortic valve prostheses: Contemporary reappraisal of mechanical versus biologic valve substitutes. Circulation 2013;128:1372-80.
9. Meller SM, Baumbach A, Voros S, et al. Challenges in cardiac device innovation: is neuroimaging an appropriate endpoint? Consensus from the 2013 Yale-UCL Cardiac Device Innovation Summit. BMC Med 2013;11:257.
10. Fanning JP, Wong AA, Fraser JF, et al. The silent and apparent neurological injury in transcatheter aortic valve implantation study (SANITY): concept, design and rationale. BMC Cardiovasc Disord 2014;14:45.
11. Fanning JP, Walters DL, Platts DG, et al. Characterization of neurological injury in transcatheter aortic valve implantation. How clear is the picture? Circulation 2014;129:504-15.
12. Spaziano M, Francese DP, Leon MD, et al. Imaging and functional testing to assess clinical and subclinical neurological events after transcatheter or surgical aortic valve replacement. J Am Coll Cardiol 2014;64:1950-63.
13. Chen Z, Mondal NK, Ding J, et al. Shear-induced platelet receptor shedding by non-physiological high shear stress with short exposure time: Glycoprotein Ib and glycoprotein VI. Thromb Res 2015;135:692-8.
14. Hu J, Mondal NK, Sorensen EN, et al. Platelet glycoprotein Ib (GPIb) ectodomain shedding and non-surgical bleeding in heart failure. Patients supported by continuous flow left ventricular assist devices (CF-LVSADs). J Heart Lung Transplant 2014;33:71-9.
15. Rodés-Cabau J, Dauerman HL, Cohen MG, et al. Antithrombotic treatment in transcatheter aortic valve implantation: insights for cerebrovascular and bleeding events. J Am Coll Cardiol 2013;62:2349-59.
16. Jamieson WR, von Lipinski O, Miyagishima RT, et al. Performance of bioprostheses and mechanical prostheses assessed by composites of valve-related complications to 15 years after mitral valve replacement. J Thorac Cardiovasc Surg 2005;129:1301-8.
17. Brennan JM, Edwards FH, Zhao Y, et al. Long-term safety

and effectiveness of mechanical versus biologic aortic valve prostheses in older patients. Circulation 2013;127:1647-55.
18. Bourguignon T, Bouquiaux-Stablo AL, Candolfi P, et al. Very long-term outcomes of the Carpentier-Edwards Perimount valve in aortic position. Ann Thorac Surg 2015;99:831-7.
19. US Patent. US4820299 Inventors: Perrier P, Lapeyre D.
20. Lapeyre D. The concept of mechanical bioprosthesis: design & materials. The Heart valve Society Meeting, Session III: Valve Replacement - Past & Future, Monaco, 8 May 2015.
21. US Patent. US5814099 Inventor: Bicer D.
22. Kini V, Bachmann C, Fontaine A, et al. Flow visualization in mechanical heart valves: occluder rebound and cavitation potential. Ann Biomed Eng 2000;28:431-41.
23. Leiria TL, Lopes RD, Williams JB, et al. Antithrombotic therapies in patients with prosthetic heart valves: guidelines translated for the clinician. J Thromb Thrombolysis 2011;31:514-22.
24. Habermann TM, Ghosh AK, editors. Mayo Clinic Internal Medicine: Concise Textbook. Boca Raton: CRC Press Taylor and Francis Group, 2008.
25. Cannegieter SC, Rosendaal FR, Briët E. Thromboembolic and bleeding complications in patients with mechanical heart valve prostheses. Circulation 1994;89:635-41.
26. Krishnan S, Udaykumar HS, Marshall JS, et al. Two-dimensional dynamic simulation of platelet activation during mechanical heart valve closure. Ann Biomed Eng 2006;34:1519-34.
27. Yoganathan AP, Corcoran WH, Harrison EC, et al. The Bjork-Shiley aortic prosthesis: flow characteristics, thrombus formation and tissue overgrowth. Circulation 1978;58:70-6.
28. Ben-Zvi J, Hildner FJ, Chandraratna PA, et al. Thrombosis on Björk-Shiley aortic valve prosthesis. Am J Cardiol 1974;34:538-44.
29. Bluestein D, Chandran KB, Manning KB. Towards non-thrombogenic performance of blood recirculating devices. Ann Biomed Eng 2010;38:1236-56.
30. Rambod E, Chandran KB, Manning KB. Towards non-thrombogenic performance of blood circulating devices. Ann Biomed Eng 2007;35:1131-45.
31. Griffith BE, Flamini V, DeAnda A, et al. Simulating the Dynamics of an Aortic Valve Prosthesis in a Pulse Duplicator: Numerical Methods and Initial Experience. J Med Device 2013;7:0409121-2.
32. Meuris B, Verbeken E, Flameng W. Mechanical valve thrombosis in a chronic animal model: differences between monoleaflet and bileaflet valves. J Heart Valve Dis 2005;14:96-104.
33. Meuris B. Research on biological and mechanical heart valves: experimental studies in chronic animal models. Verh K Acad Geneeskd Belg 2002;64:287-302.

Cite this article as: Scotten LN, Siegel R. Are anticoagulant independent mechanical valves within reach—fast prototype fabrication and *in vitro* testing of innovative bi-leaflet valve models. Ann Transl Med 2015;3(14):197. doi: 10.3978/j.issn.2305-5839.2015.08.18

Supplementary materials

Methods and materials

In this study we used a modified pulse duplicator for valve testing described previously (1-3). Test conditions included: pulse rate 70 beats/min; ~average peak instantaneous forward flow rates 27 L/min (mitral) and 35 L/min (aortic) appropriate to mechanical valve insufficiency of typically ~12% and cardiac output of ~5 L/min. The test fluid was saline with viscosity 1 mPa·s and density 1.0 g/mL.

Valves tested

Figure S2 shows photographs (BVs and BV_{3D}) and a CAD rendition (middle panel) of the prototype valves.

Prototype bi-leaflet valves BVs

In our study, overall valve kinematics was important but valve occluder motion at closure was of particular interest. We surmised that valve motion is influenced by pulsatile flow profile but influence of valve geometric parameters needed examination. A total of 56 prototype BV valves were tested for lowest TPI.

In *Figure S1*, some of the geometric parameters considered for BV design potential exploration were: valve profile (A), leaflet length (B), fulcrum site location (C1, C2), leaflet inflow/outflow aileron angles (Di, Do), symmetric/asymmetric inflow/outflow wing curvatures (E1, e2, e3, e4), aileron length (F), wing: center location (G), height (H), width (J), housing/leaflet pivot location (K), leaflet surface texture (L). Combinations of these variables were used in a number of prototype BV valves to optimize for lowest TPI. Additionally, we assessed unique valve movements induced by fluid mechanical factors such as: lift, drag, stall, vortex shedding, torque, mechanical advantage and boundary layer profiles, all of which can affect TPI. In a description of experimental modifications to a SJM bi-leaflet mechanical valve, Murphy and co-workers offered examples from the biological world and from man-made technologies such as: leading edge tubercles, jet nozzle modifications, and vortex generators to suggest how improvements in valve performance may be possible (34). Therefore, additional geometric parameters not described herein may require exploration to achieve final design optimization. Leonardo Technology was able to assess unique valve movements induced by the above fluid mechanical factors.

Expeditious construction of experimental prototype valves was essential. Simplified fabrication techniques were developed to allow complex valve shapes to be made, tested, and documented at a rate of ~2/day. Various traditional subtractive manufacturing techniques were used for material removal including: lathe and milling tools, metal snips, files and abrasive papers. The housing was made from equal half-sections of Delrin™ held together with a friction-fitted aluminum ring. The half housing expedited trial fit up and assemblage. Occluders were made from ~0.41 mm brass sheet. Self-adhesive labels were Ink-jet printed and occluder outlines were CAD drawn using Visio™. Labels were then applied to brass sheet, rough cut with snips and filed to final boundary. Bending was done manually while clamping the brass leaflet in a vise appropriate to the bend mark. Copper wire axles (~0.81 mm diameter) and open stops were sited specific to purpose and soldered to the brass. Balsa wood was rough-cut prior to attachment to the brass with ethyl cyanoacrylate (Loctite™ 401). The balsa was hand sculpted using various abrasive tools and waterproofed with lacquer.

3D printed (BV_{3D})

Additive technologies, also called 3D printing, is a process whereby successive layers corresponding to virtual computer assisted design (CAD) models automatically combine to build up the final part (*Figure S2*, right). The printed valve was made from white acrylonitrile butadiene styrene (ABS) with printer-produced resolution of ~0.10 mm. Reduced surface roughness was achieved by abrasion with fine materials sufficient to provide low friction occluder function. Four brass rods (0.81 mm diameter each) positioned in holes drilled into occluder and housing provided pivot points. TPI is highly dependent on total closed valve leakage area mandating close attention to manufacture and final fit-up of the high tolerance components.

Control valves and patented early prototype mechanicals from other investigators

Edwards-Perimount™ Model 2800 pericardial valve, (Edwards Lifesciences Inc., Irvine, California, USA) and St Jude Medical, Regent™ mechanical valve (St. Jude Medical, St. Paul, Minnesota, USA). *Table S1* gives approximate dimensional specifications for the valves tested. The complementary (non-test) valve was a Mitroflow 29 mm pericardial valve (Sorin S.p.A., Milan, Italy). Also compared are the tri-leaflet Lapeyre-Trifo (L-T) (19,20) and the bi-leaflet Bicer (21).

Synchronization of data

Realistic flow source impedance was provided by the combination of pulse duplicator model ventricle/piston

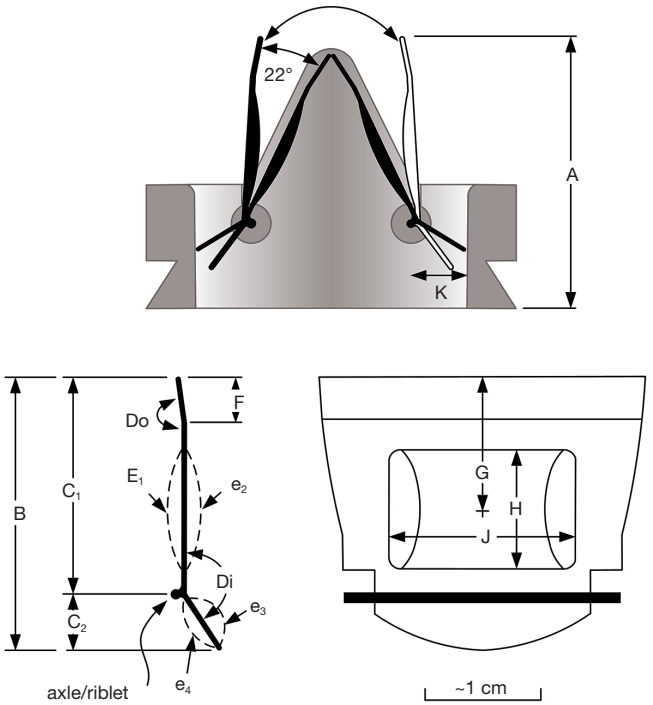

Figure S1 Geometric variables in BV designs considered.

Table S1 Approximate valve dimensions

Valve	~ID_{MAX}[†] (mm)	~TAD[‡] (mm)	Profile (mm)	
			Open	Closed
Mechanical BV prototypes				
BV_{3D}	24	27	21	18
BVs	24	27	24	23
Control valves				
SJM Regent™	23	25	15	12
Perimount™	23	25	17	17
Other mechanical valves				
L-T	23	28	16	10
Bicer	24	27	13	10

[†], internal diameter maximum; [‡], tissue annulus diameter.

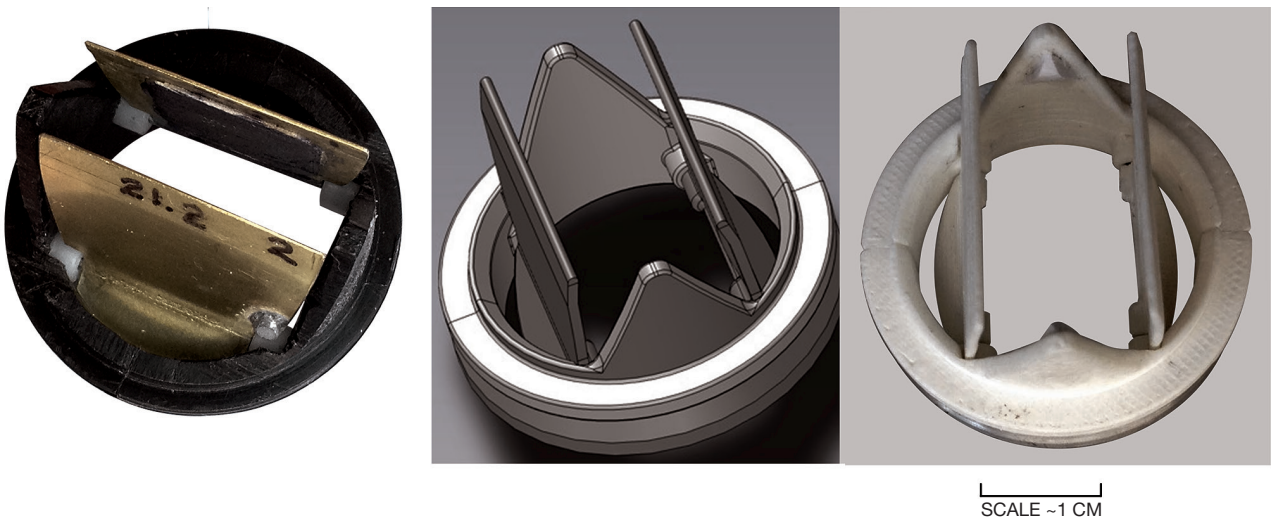

Figure S2 Prototype bi-leaflet mechanical valves. BVs, model #21.2 (left), CAD rendering of BV_{3D} (middle), BV_{3D} printed (right).

pump/Viscoelastic Impedance Adapter (VIA model 7991, ViVitro Labs Inc., Victoria, BC, Canada). VIA has been described previously (2). Importantly, it simulates visco-elastic and isovolumetric functionality, a physiologic attribute which influences ventricular pressure rates (dp/dt) and other dynamic profiles. Because of inherent pulse duplicator/VIA reactive properties, the acquired data from experiments necessitated post experiment synchronization. Since data phasing was dependent on valve and test conditions, T_{REF} mitigated this problem by providing a stable reference time. In *Figure 1* (upper panel) T_{REF} coincides at the zero (0) mL/s crossover point on the volumetric flow rate profile just prior to the test valve closure. Specific to each valve, profiles are made synchronous to T_{REF}.

Calculation of TPI

To identify the parameters in the equations, refer to *Figure 1*.

TPI α $(A + B + C) \div 3$

A. Ratio of valve geometric open area at peak forward flow (A_{PF}) relative to area at zero forward flow rate (A_{0F}).
   $= A_{PF}/A_{0F}$ (control valve) $\div A_{PF}/A_{0F}$ (test valve)
   A_{PF}: is the PDVA at peak forward flow rate (ideal value >2.3 cm^2);
   A_{0F}: is the PDVA at zero forward flow rate just prior to valve closure (ideal value zero cm^2).

B. Test valve derived mean negative Regional Backflow Velocity (RBV_{-MEAN}) ÷ control valve RBV_{-MEAN}
   where: RBV_{-MEAN} = (valve volumetric flow rate, mL/s ÷ PDVA, cm^2)$_{-MEAN}$

C. Range of variation (maximum - minimum) for RBV_{-MAX}, cm/s
   RBV_{-MAX} (for test valve) ÷ RBV_{-MAX} (for control valve)

Note: Quantities A, B, and C were obtained for 10 consecutive cycles.

In the above equations, A, B and C are each contributory to the TPI. However, their relative importance or "weighting" is unknown. In this study, in order to achieve a simple and practical ranking system, we assigned equal weight to each resulting in a number representing the average of all three. In *Figure 3*, promising specific prototype valves that produced low TPI values merit consideration for further development and study. The majority of experiments were performed in the aortic site but site dependent differences have been noted.

Leonardo^{VSI} technology

Current summary of technical specifications (1-3):

- Temporal resolution ≈1.04 µs;
- Spatial area resolution (closed valve), 0.001 cm^2 (n=10 cycle average);
- Telecentric lens maintains constant magnification ≈0.16×;
- Working distance ≈18 cm (AORTIC); ≈19 cm (MITRAL);
- Perspective error <0.3% (depth 15 mm);
- Spatial sensitivity variation <6%;
- Typical site dependent linear calibrations are:
  y=0.00128x, with R^2 =0.99988 (AORTIC);
  y=0.00132x, with R^2 =0.99959 (MITRAL);
- LED back light (diffuse red):
  Wavelength 625±15 nm;
  Uniformity 99.24%;
  Luminance 5,780 cd/m^2.

References

34. Murphy DW, Dasi LP, Vukasinovic J, et al. Reduction of procoagulant potential of b-datum leakage jet flow in bileaflet mechanical heart valves via application of vortex generator arrays. J Biomech Eng 2010:132;071011.